Electrolysis of low-grade and saline surface water

Wenming Tong[1], Mark Forster[2], Fabio Dionigi[3], Sören Dresp[3], Roghayeh Sadeghi Erami[1], Peter Strasser[3]*, Alexander J. Cowan[2]* and Pau Farràs[1]*

1. School of Chemistry, Energy Research Centre, Ryan Institute, National University of Ireland Galway, Galway, Ireland.
2. Department of Chemistry, Stephenson Institute for Renewable Energy, University of Liverpool, Liverpool, UK.
3. The Electrochemical Energy, Catalysis and Materials Science Laboratory, Department of Chemistry, Chemical Engineering Division, Technical University Berlin, Berlin, Germany.
*e-mail: pstrasser@tu-berlin.de; a.j.cowan@liverpool.ac.uk; pau.farras@nuigalway.ie

Abstract

Powered by renewable energy sources such as solar, marine, geothermal and wind, generation of storable hydrogen fuel through water electrolysis provides a promising path towards energy sustainability. However, state-of-the-art electrolysis requires support from associated processes such as desalination of water sources, further purification of desalinated water, and transportation of water, which often contribute financial and energy costs. One strategy to avoid these operations is to develop electrolysers that are capable of operating with impure water feeds directly. Here we review recent developments in electrode materials/catalysts for water electrolysis using low-grade and saline water, a significantly more abundant resource worldwide compared to potable water. We address the associated challenges in design of electrolysers, and discuss future potential approaches that may yield highly active and selective materials for water electrolysis in the presence of common impurities such as metal ions, chloride and bio-organisms.

Freshwater is likely to become a scarce resource for many communities, with more than 80% of the world's population exposed to high risk levels of water security[1]. This has been recognized within the Sustainable Development Goal 6 (SDG 6) on Clean Water and Sanitation[2]. At the same time, low-grade and saline water is a largely abundant resource which, used properly, can address SDG 7 on Affordable and Clean Energy as well as SDG 13 on Climate Action. Hydrogen, a storable fuel, can be generated through water electrolysis and it may provide headway towards combating climate change and reaching zero emissions[3], since the cycle of generation, consumption and regeneration of hydrogen can achieve carbon neutrality. In addition to providing a suitable energy store, hydrogen can be easily distributed and used in industry, households and transport.

Hydrogen, and the related fuel cell industry, has the potential to bring positive economic and social impacts to local communities in terms of energy efficiency and job markets; globally the hydrogen market is expected to grow 33% to US$155 billion in 2022[4]. However, there are remaining challenges related to the minimization of the cost and integration of hydrogen into daily life, as well as meeting the ultimate hydrogen cost targets of <US$2 kg^{-1} set by the US Department of Energy[5–7].

Commercially available water electrolysers operate with support from ancillary components/equipment[8,9]. The high purity water feeds are achieved by incorporating extensive water purification systems into the overall electrolyser design (internal) or via pre-treatment using external

purification/desalination plants. Desalination and subsequent purification and the associated investment costs for plantation, land, maintenance and transportation, therefore impose considerable costs. Several techno-economic studies have been published in the past few years[10,11], however, a more comprehensive review with up-to-date costs is still needed. Desalination costs vary considerably depending on the price of electricity, and increase if intermittent renewable sources are used[12]. Nevertheless, the cost of water purification systems remains significant[12]. Particular interest in direct saline water electrolysis exists for off-shore large-scale hydrogen production, a sector where the capital costs are dominated by the footprint of the installation, and the simplification in engineering by removing pre-treatment systems would have a great impact on the economic viability of such installations[3].

A route to reduce cost would be to use low-grade or saline water directly through development of efficient and selective catalytic electrode materials and the utilization of effective membranes in the electrolysers that are suitable for impure water. Therefore, ideal catalytic electrode materials and membranes should be able to deal with competing redox reactions at both electrodes, complications related to membrane function, reactor degradation and biofouling. Here we review key issues and recent research in electrolysis and the development of electrode materials/catalysts targeting direct use of low-grade and saline water in the electrolysis processes. In addition, we address the major aspects in the design of electrolysers for hydrogen generation.

Challenges of saline water electrolysis

Splitting water into oxygen and hydrogen is an energetically uphill chemical process where an external energy source is required to drive the reaction. In an electrolyser, electricity is converted to, and stored in the form of, chemical bonds. The hydrogen evolution reaction (HER) at the cathode is a two electron-proton reaction, which can be formulated as Eqs. (1) or (2) under acidic or alkaline conditions, respectively.

$$\text{Acidic} \qquad 2H^+ + 2e^- \rightarrow H_2 \qquad (1)$$

$$\text{Alkaline} \qquad 2H_2O + 2e^- \rightarrow H_2 + 2OH^- \qquad (2)$$

The counter reaction at the anode, the oxygen evolution reaction (OER), is a multi-electron transferring process, involving several intermediates and the removal of four protons per oxygen molecule evolved. It can be described by Eqs. (3) or (4) in acidic or alkaline environments, respectively.

$$\text{Acidic} \qquad 2H_2O \rightarrow 4H^+ + O_2 + 4e^- \qquad (3)$$

$$\text{Alkaline} \qquad 4OH^- \rightarrow 2H_2O + O_2 + 4e^- \qquad (4)$$

Catalysts are usually either deposited onto the current collector electrodes (catalyst coated electrode, CCE) or are coated directly onto the ion exchange membranes (catalyst coated membrane, CCM) to

facilitate the water splitting reactions. An important catalytic activity metric is the difference between the applied potential at a given current density and the half-reaction standard potential; the so called overpotential (η). This difference characterizes the extra energy taken to push the half reaction significantly forward from the thermodynamic zero net-current equilibrium point[13]. The complexity of the OER requires a large overpotential, even with state-of-the-art catalysts and especially when compared to the HER.

Water electrolysis typically requires ultra-purified water, either directly in membrane electrolysers (proton exchange membrane water electrolysers, PEMWE; anion exchange membrane water electrolysers, AEMWE) or in a mixture with salts for alkaline water electrolysers (AWE). The key challenges in the direct electrolysis of saline water have long been identified and discussed[14], and remain major issues today. Although carbonates in seawater (saline water) can act as buffers, the capacity is not high enough to prevent increases in the local pH at the cathode and decreases in the local pH at the anode. Studies showed changes in pH near the electrode surface could be on the order of 5–9 pH units from that of the bulk seawater, for a slightly buffered medium when its overall pH value is in between 4 and 10, even at moderate current densities <10 mA cm^{-2}(ref. [15–17]). Such dramatic pH fluctuations may cause catalyst degradation. Local pH increases near the cathode during seawater (not artificially buffered) electrolysis can lead to precipitation of magnesium hydroxide ($Mg(OH)_2$), which occurs when pH ≥ ~9.5(ref. [18]), blocking the cathode[14,19]. Stabilization of pH fluctuations may require the addition of supporting electrolytes[20,21].

Other challenges include the presence of non-innocent ions (both anions and cations)[17,22] and bacteria/microbes[23], as well as small particulates, all of which may poison electrodes/catalysts and limit their long-term stability. This challenge also extends to the membranes used for the separation of the anode and cathode[24]. Another key issue to consider is the competition between the OER and chloride chemistry at the anode.

Chloride electro-oxidation chemistry is complicated and several reactions occur depending on the pH values, potentials applied and temperature. If, for simplicity, we consider the temperature of 25 °C and fix the total concentration of chlorine species to 0.5 M (a typical chloride concentration for seawater), a Pourbaix diagram for aqueous chloride chemistry can be constructed as shown in Fig. 1[17].

When the pH is below 3.0 the free chlorine evolution reaction (ClER, Eq. 5) dominates over the other chloride oxidation reactions (Fig. 1). Hypochlorous acid formation might also occur at lower pH at high anodic potentials, but becomes the major reaction for pH 3–7.5. Hypochlorite formation takes place at pH values higher than 7.5 (Eq. 6), which represents the pK_a of hypochlorous acid. Partial dissociations (that is, chlorine dissolved in water) and disproportionation (that is, hypochlorite ions subjected to higher temperature) complicate the chemistry of chlorine species. At the two pH extremes the two chloride oxidation reactions are:

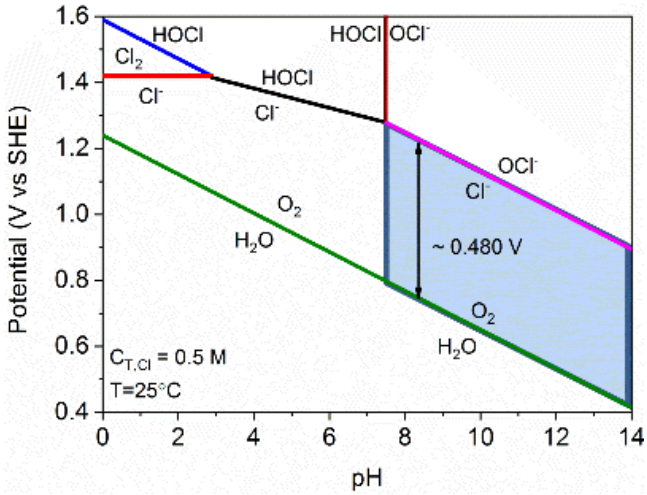

Fig. 1 The Pourbaix diagram of an aqueous saline electrolyte. Represented is the electrode potential versus pH diagram, it provides information of the stability of an aqueous 0.5 M NaCl electrolyte, including the H_2O/O_2 and the $Cl^-/Cl_2/HOCl/ClO^-$ redox couples. The diagram depicts potential–pH regions where the oxygen evolution reaction (OER) and the chloride oxidation reactions are thermodynamically possible. The green line represents the thermodynamic equilibrium between water and oxygen. At electrode potentials more positive than the green line, the OER process becomes thermodynamically possible. The red line shows the competing acidic oxidation of chloride to free gaseous chlorine. The black and purple lines mark the onset of the oxidation of chloride to hypochlorous acid, HClO, or hypochlorite, ClO^-. The potential difference between the chloride chemistry and the water oxidation is maximized to 480 mV in alkaline media pH > 7.5 (light blue region), where chloride is oxidized to ClO^-. SHE, standard hydrogen electrode. Adapted with permission from ref. [17], John Wiley and Sons.

ClER:

$$2Cl^- \rightarrow Cl_2 + 2e^- \qquad (\mathbf{E^0}= 1.36\ \text{V vs. SHE, pH=0}) \qquad (5)$$

Hypochlorate formation:

$$Cl^- + 2OH^- \rightarrow ClO^- + H_2O + 2e^- \qquad (\mathbf{E^0}= 0.89\ \text{V vs. SHE, pH=14}) \qquad (6)$$

The competing chloride oxidations are thermodynamically unfavourable compared to the OER (Fig. 1) and the difference between the standard electrode potentials increases with increasing pH until the hypochlorite formation starts, where it remains at its maximum value of ~480 mV (ref. [17]). In other words, under alkaline conditions a water oxidation catalyst can exhibit up to 480 mV kinetic overpotential without any interfering chlorine chemistry. This is known as the 'alkaline design criterion' in saline water electrolysis[17], because the requirements for the catalytic activity of the OER catalyst are least stringent in this region.

It is worth noting that both chloride reactions (Eqs. (5) and (6)) are two-electron reactions, in contrast with the OER in which four electrons are involved. This difference in the numbers of electrons involved in the mechanisms (Eq. (2) versus Eq. (4)) give rise to the commonly observed higher overpotential for OER than chloride oxidation and makes OER kinetically unfavourable. Therefore, developing highly selective anode catalysts is essential to avoid the evolution of corrosive and toxic chlorine gas during the electrolysis of saline water.

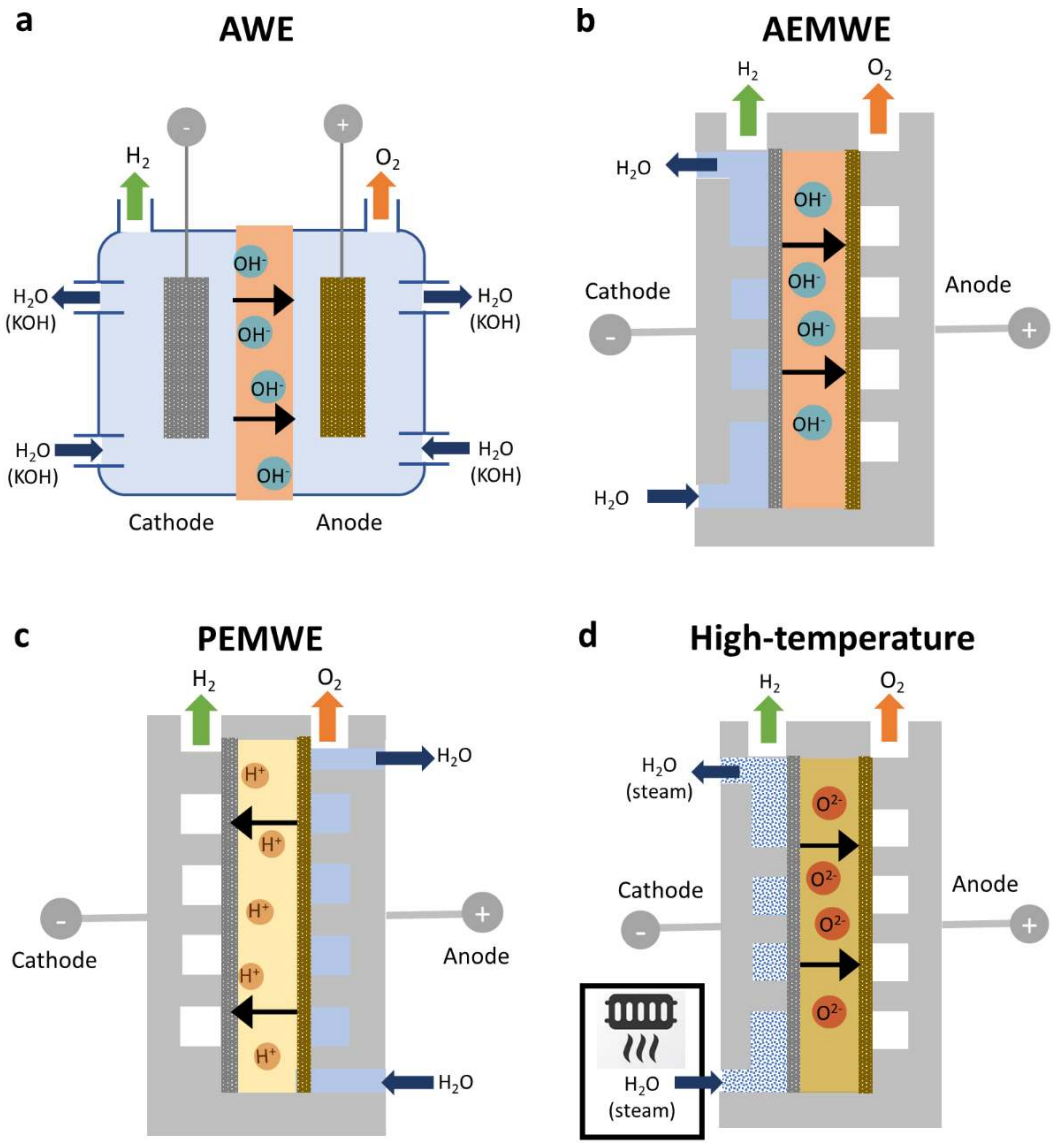

Fig. 2 Leading configurations for water electrolysis. a, An alkaline water electrolyser (AWE) operates as a 2-compartment cell in which a liquid alkaline electrolyte (typically 20–30% KOH) is pumped around both sides and a porous diaphragm allows hydroxyl ion (OH^-) migration while preventing gas crossover. **b**, An anion exchange membrane water electrolyser (AEMWE) sandwiches an OH^- transporting membrane between the anode and cathode. Water is supplied to the cathode in this example, however it is also possible to supply water to the anode or both sides. **c**, A proton exchange membrane water electrolyser (PEMWE) consists of a solid acid electrolyte polymer sandwiched between the anode and cathode. In most cases, water is only fed to the anode. **d**, High-temperature water electrolysers include proton conducting ceramic electrolysis (~150–400 ºC) and solid oxide electrolysis (~800–1000 ºC). Water evaporates and transports to the cathode as steam to produce H_2 while a solid oxide or ceramic membrane transports O^{2-} to the anode.

Reactor design considerations

Currently the two proven low-temperature (<100 °C) water electrolyser technologies dominating the commercial market are AWE and PEMWE[25]. Other emerging technologies include low temperature AEMWE[26], as well as high-temperature electrolysis, such as proton conducting ceramic electrolysis (~150 °C–400 °C)[27] and solid oxide electrolysis (~500–800 ºC)[28]. These four configurations are depicted in Fig. 2.

These electrolyser technologies use either ultra-pure, deionized 18.2 MΩ·cm water or 20–30% KOH aqueous solution (AWE) with contaminants at and below the ppm level. Such high levels of water purity are chosen to avoid complications related to catalyst operation, membrane operation and general component degradation. The severity of the challenges associated with use of impure water depends to some degree on the electrolysis configurations.

PEMWE contain a solid acid polymer electrolyte[29] (for example, Nafion) between the anode and cathode. In most cases, the water feed is only supplied to the anode, where it is oxidized to form O_2 and H^+. Protons then migrate through the PEM towards the HER catalyst (cathode). In this approach, the low pH medium provided by the PEM complicates the anode chemistry and OER selectivity over chloride oxidation reactions becomes challenging. In addition, as a type of cation transporter, the commonly used Nafion membrane is vulnerable to foreign ions, especially cationic impurities, which can be trapped and concentrated, leading to a reduction in proton conductivity[25,30]. The PEM may isolate certain impurities at the anode, however cationic species such as metal ions and Mg^{2+} will still migrate from the anode to reach the cathode. It is possible to feed water only to the cathode thus minimizing any interaction between chloride ions and the anode. In this case water migrates through the membrane where it is oxidized, protons transfer back to the cathode where H_2 is produced[31]. However, migration of electrolyte and impurities towards the anode will still occur to some degree. Due to transport through the membrane both configurations are likely to result in contact between impurities and the cathode, potentially leading to metal or salt deposition.

An AWE operates as a two-compartment cell separated by a porous diaphragm that allows hydroxyl ion (OH^-) migration while preventing gas crossover. A liquid alkaline electrolyte is pumped around both sides of the cell and water is reduced at the cathode into H_2 and OH^-. OH^- then migrates through the diaphragm towards the anode where O_2 formation occurs. Diaphragm materials for AWE, such as Zirfon, are reported to be more physically robust and less susceptible to blockages compared to membranes (PEM/AEM)[32]. In contrast to PEM and AEM that largely block either anions or cations, respectively, both types of species, such as H^+, Na^+, OH^- and Cl^-, are able to migrate through the diaphragm, which should be kept in consideration for system design. This may be problematic if it lowers the transference numbers of the most mobile ions.

In an AEMWE, the anion exchange membrane is sandwiched between the anode and cathode. Water can be supplied to the cathode, the anode or both sides. H_2 and OH^- are generated at the cathode and OH^- migrates through the membrane to the anode where O_2 is produced[26]. The membrane itself shares the same limitations with that of AWE related to unwanted migration of anions such as Cl^-, meaning competition between OH^- and Cl^- oxidation is a concern regardless of where the electrolyte is fed[21]. The high operating pH of both AWE and AEMWE can help to minimize Cl^- oxidation, making them particularly interesting for saline water splitting.

High-temperature water electrolysers include proton conducting ceramic electrolysis (~150–400 °C) and solid oxide electrolysis (~800–1000 °C). Water evaporates and transports to the cathode as steam to produce H_2. A solid oxide or ceramic membrane selectively passes O^{2-} through to the anode to form O_2[28]. This configuration may provide an opportunity to purify the water source (generating 'clean' steam) before it reaches the catalyst and membrane[33]. Therefore, this technology has the potential to open up the design window beyond electrode materials that are investigated in the other technologies. However, the high operating temperature means a higher energy demand and a higher operational cost compared to rival technologies that typically operate below 100 °C. In addition, the high temperature limits the type of electrode materials and other electrolyser components to meet the stability requirements for long-term operation. These challenges may prevent their potential installation in offshore facilities coupled to large-scale wind farms, making them more suitable for coastal installation.

All four configurations share common problems including physical blockages from solid impurities, precipitates and microbial contaminations affecting either the catalysts or separator material. Thus, a simple filtration of the saline or low-grade water feeds is essential for avoidance of membrane blockages. It may be possible to maintain membrane activity through recovery procedures. For example, periodically resting an electrolyser at open circuit has been shown to recover a portion of lost activity assigned to chloride blocking of the membrane[21]. Metal components are also at risk of corrosion. For example, in a PEM electrolyser the current collectors and separator plates are typically made of titanium, graphite or a coated stainless steel[25], and the lifetime of these materials, particularly in the presence of Cl^-, should be carefully considered.

The chlor-alkali industry can provide some guidance for selecting materials capable of withstanding harsh corrosive environments. Because of its high stability, titanium is chosen for all parts that are in contact with chlorinated water, including the support materials for anode and cathode catalysts. The corrosion resistance of titanium relies on the development of a surface oxide layer. Other useful components used in this industry are Teflon that can be found as a construction component thanks to its inertness, and persulfonated membranes such as Nafion to separate half-cell reactions. However, they are still susceptible to physical damage[34,35]. To circumvent some of the aforementioned issues, recent studies have shown an interest towards using water vapour (including saline water) as water feeds in both PEMWE and AEMWE[36–38]. In these cases, air was bubbled through a saline aqueous media to reach high levels of humidity and gas phase electrolysis was conducted. A system composed of buoys that are floating at the ocean surface has been proposed[36], which has the benefit of overcoming the risk of fouling of catalysts and membranes associated with impure liquid water, although the current density is significantly lower than that for liquid-based electrolysers.

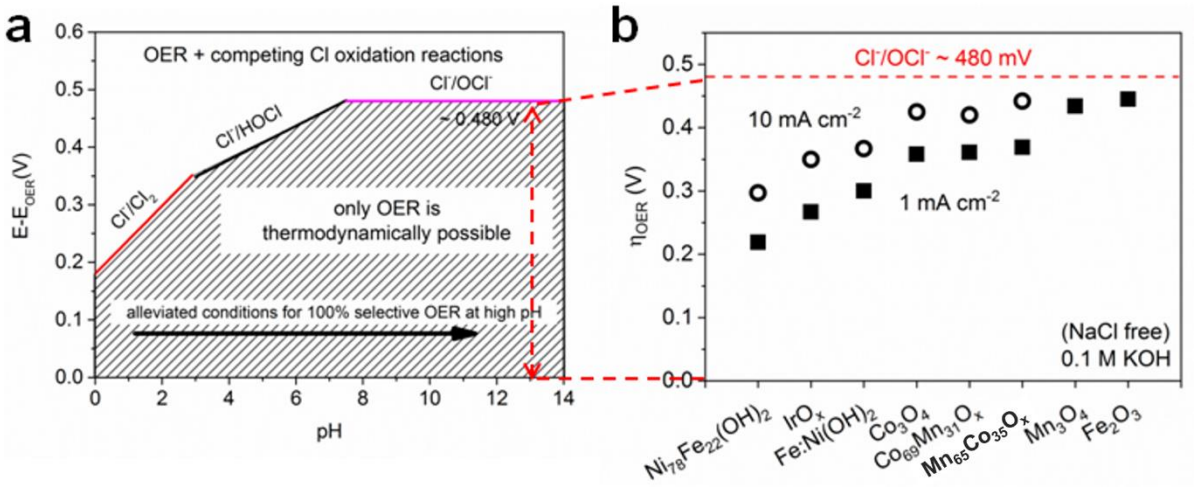

Fig. 3 Experimental implementation of the alkaline design criterion of saline water splitting. a, Predicted maximally allowed kinetic overpotentials (derived from thermodynamic Pourbaix diagrams) of an OER electrocatalyst as a function of pH to realize 100% selective water splitting. **b**, Experimental OER overpotentials of supported oxide catalysts in O_2 saturated 0.1 M KOH compared with reference IrO_x/C catalyst evaluated at the current density of 1 mA cm^{-2} (full symbols) and 10 mA cm^{-2} (open symbols). The red dashed lines show the overpotential limit in alkaline conditions (alkaline design criterion) of ~480 mV. While many catalysts fulfil the design criterion at low current densities (1 mA cm^{-2}), this becomes challenging for moderately higher current densities such as 10 mA cm^{-2}. Mn_3O_4 and Fe_2O_3, for instance, no longer fulfil the design criterion at 10 mA cm^{-2} and hence would start generating detrimental ClO^- by-products. Panel **a** is adapted with permission from ref. [17], John Wiley and Sons; panel **b** summarizes data reported in refs. [17,20].

Anode materials for electrolysis in impure water

Several strategies have been devised for OER-selective water oxidation anode catalysts that operate in low-grade or saline water. First, the alkaline OER/ClER design criterion has been leveraged, that is, maximizing the thermodynamic potential difference between the two catalytic processes by operating the electrolyser in alkaline conditions. This implies the development of highly active OER catalysts designed for alkaline conditions that provide the desired Faradaic current at or below 480 mV. The second strategy is the design of OER catalysts for alkaline or acidic environments with exclusive selectivity towards the OER due to surface sites of optimized binding of OER intermediates. Third, Cl^- blocking layers next to the OER catalyst have been used to prevent the diffusion of Cl^- ions from the electrolyte to the surface of the OER catalyst. This Cl^- blocking layer may operate in alkaline or acid conditions.

Alkaline design criterion. The first approach is based on thermodynamic and kinetic considerations, as well as the fact that saline water is essentially a non-buffered electrolyte. Therefore, an additive is likely required to avoid changes in local pH during electrolysis. Kinetic considerations suggest that it is particularly challenging to compete with chloride oxidation due to the more complicated catalytic four-electron mechanism of the OER, while thermodynamics indicates that alkaline conditions provide a larger potential window where OER is favourable. Based on these reasons, an alkaline catalyst design

criterion (Fig. 3a) was proposed to achieve 100% OER selectivity in saline water splitting at alkaline pH, provided the overpotentials of the catalysts are lower than ~480 mV at the desired current density (for example, 500–2000 mA cm^{-2})[17].

It is often difficult to achieve the desired high current densities below an overpotential of 480 mV (Mn_2O_3 and Fe_2O_3 in Fig. 3b)[20]. As an additional 'criterion', the overpotential should ideally be as moderate as possible so that it is still less than 480 mV for a given high current density. High performances in Cl^--free 0.1 M KOH and 1 M KOH electrolytes have been reported for the family of NiFe oxyhydroxide catalysts[17,39,40], which include some of the most active catalysts in alkaline media. An unsupported NiFe layered double hydroxide (LDH) catalyst in a membrane electrode assembly (MEA) experimentally confirmed the concept of the criterion, by demonstrating current densities up to 290 mA cm^{-2} at under ~480 mV overpotential, which is close to what is required for medium or large size electrolysers[21]. The performance loss after 100 hours to about 50–70% of the initial activity was attributed to the unsuitability of the membrane rather than to catalyst degradation, which was supported by quasi in situ XAS measurements.

As shown in Fig. 4a, FeO_x nanomaterials as bifunctional HER/ OER catalysts were reported to exhibit OER activity in alkalinized saline water with comparatively lower performances (overpotential of 400 mV at 10 mA cm^{-2})[41]. However, such bifunctional HER/ OER activities allow an overall precious-metal-free electrolyser to be realized. Formation of surface redox-active species (iron phosphate) led to significant increases in both catalytic performance and stability in the case of phosphate buffered saline water oxidation by $CaFeO_x$ at pH 7.0 (Fig. 4b)[42]. Recently, nickel oxide electrodes were also successfully used in alkalinized saline water with 100% OER selectivity[43].

Selective OER sites and reaction environments. The second approach aims to develop catalysts containing active sites that optimize the chemical bonding of the reactive OER intermediates to make them highly OER selective. This approach is feasible in all pH media but challenging at the same time since the sites of OER active catalysts are typically also active for the ClER[44]. This issue was addressed in several theoretical studies. Calculations on various rutile (110) oxide surfaces confirmed that a linear scaling relationship between the Cl and O adsorption energies exists. This implies that the ClER always requires lower overpotentials than the OER where the scaling holds[45]. One report showed that on a RuO_2 (110) surface the kinetic volcano plot of the ClER is flatter than that of the OER[46], which was related to the number of intermediates. The tips of both volcano plots are very close and for this reason as well as the predictions of linear scaling relationships, it is not feasible to improve the OER selectivity where it dominates over ClER. Fundamentally, new types of sites are necessary to break the scaling relationships and so to enable sites with higher OER selectivity.

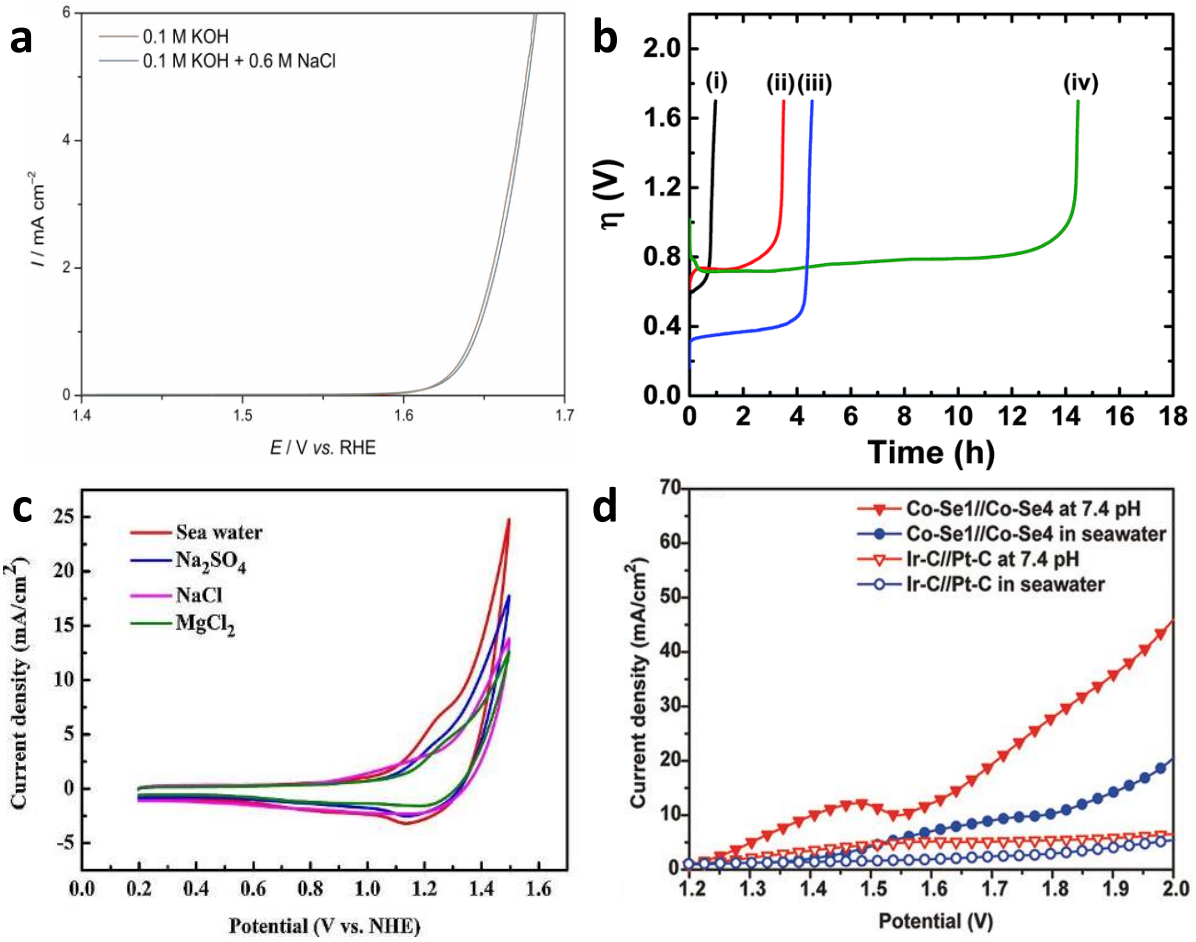

Fig. 4 Water oxidation activity and stability of oxide catalysts and influence of anionic and cationic contaminations. a, OER selectivity in alkaline artificial seawater electrolyte solution. Linear sweep voltammetry (LSV) of a FeO_x electrode operated in 0.1 M KOH and (0.6 M NaCl + 0.1 M KOH) electrolytes. **b**, Overpotential transients of different materials, FTO|Co–Pi (i), FTO|FeO_x (ii), FTO|IrO_x (iii) and FTO|$CaFeO_x$|$FePO_{4(25)}$ (iv), at 10 mA cm^{-2} in phosphate buffered (0.5 M, pH 7) saline water under N_2 atmosphere. **c**, CVs of Co–Fe LDH on a glassy carbon electrode in saline water and aqueous solutions including $MgCl_2$, NaCl or Na_2SO_4 as electrolytes. Scan rate: 100 mV s^{-1}. **d**, Polarization curves of Co–Se_1//Co–Se_4 and Ir–C//Pt–C in buffered saline water at a scan rate of 5 mV s^{-1}. The counter and reference electrodes were Pt mesh and Ag/AgCl respectively. iR compensation was used. Panel **a** reproduced with permission from the supporting information of ref. [41], John Wiley and Sons. Other figures reproduced/reprinted with permission from ref. [42], Royal Chemical Society (**b**); ref. [48], Elsevier (**c**); and ref. [49], John Wiley and Sons (**d**).

Experimental investigations of OER selective saline water splitting catalysts have focused on Co and Ru based systems. Co-based OER catalysts are subjects of intense investigations due to their performance at neutral pH with presence of a phosphate buffer. This is particularly appealing for saline water oxidation as the average pH of saline water is close to neutral. Co–Pi, an electrodeposited Co-based catalyst from a phosphate electrolyte, can sustain selective OER in phosphate electrolyte containing 0.5 M NaCl (pH 7.0) at 1.30 V (versus normal hydrogen electrode (NHE)), corresponding to ~483 mV overpotential at current densities comparable to NaCl-free electrolyte (greater than 0.9 mA cm^{-2}). Only 2.4% of the charge passed in a 16 h experiment was attributed to oxidized chloride species[47].

When mixed with Carbon (Vulcan XC-72) and deposited on Ti mesh electrodes, Co–Fe LDH nanoparticles exhibited a Faradaic efficiency of 94 ± 4% in simulated saline water (3.5% salinity, pH = 8.0). Only 0.06% of the total charge passed was attributed to oxidized chloride species after an 8 hours controlled potential experiment at a constant overpotential of 560 mV[48]. The improved OER performance in saline water was attributed to a synergistic effect of the multiple ions contained in saline water and CoFe LDH (Fig. 4c), that is, complex multiple ions in seawater can mediate proton transfers in concert with electron-transfer reactions[48]. Co-based selenide electrodes obtained by selenization of Co foils were also tested in phosphate buffered saline water (pH= 7.09), with superior performance to the reference Ir–C/Pt–C (Fig. 4d)[49]. These examples highlight the relevance of operating at the condition close to the neutral/ alkaline design criterion to achieve high OER selectivity. The concept of tuning the relative reaction rates of key steps of the OER and the chloride oxidation reactions is an important strategy toward OER selective sites or site environments. For instance, the use of non-innocent elements such as iron and selenium can facilitate proton transfer on the reactive interfaces. However, the fundamental mechanistic origin of these observations in saline water still await further clarification.

Ru based catalysts have shown selectivity for both OER and ClER. While most of the Ru based studies had a focus on the ClER[35,50–53] or the fundamental understanding of the ClER on ruthenium titanium oxide (RTO)[46,54–56], there are a few studies that reported enhanced selectivity towards OER on some Ru-based catalysts. Some speculated that doping of Zn into RuO_2 crystal structure caused a rearrangement of the local atomic structure in the vicinity of the Zn ions, enhancing the oxygen evolution process at positive potentials and, overall, improving the selectivity of the OER in chloride containing acidic media[57]. Additional work is required to confirm and clarify the origins of the enhanced OER selectivity in all the above experimental reports. This involves state-of-art and novel emerging in situ and operando electrocatalytic studies of the structure and chemical state of the catalytic interface during the catalysis, combined with time-resolved studies of the OER and ClER reaction product onset and formation rates[58–61].

For a different system, density functional theory calculations have predicted transition metal hexacyanometallates (MHCMs), such as Prussian blue (PB, $Fe_4[Fe(CN)_6]_3 \bullet nH_2O$) and its analogues to be highly energy efficient and selective OER catalyst materials[62]. In this context, a thin shell of MHCM provides good catalytic activity while the conductive core of basic cobalt carbonate (BCC) facilitates efficient charge transfer. This material in a triple-junction solar cell achieved 17.9% solar to hydrogen conversion efficiency in saline water at neutral pH. The addition of NaCl (50 mM NaCl, 0.1 M phosphate buffer at pH 7.0) into the electrolyte enhanced the water oxidation rate by Ru(II) polypyridyl complexes[63].

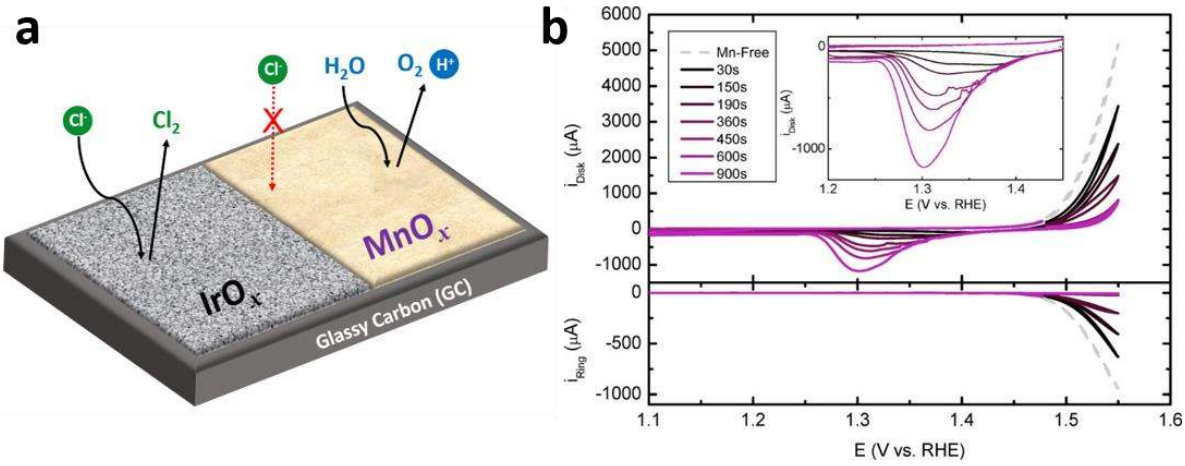

Fig. 5 Selective OER catalysts by Cl^- blocking overlayers. a, Illustration of MnO_x deposited onto IrO_x decreases the ClER selectivity in the presence of 30 mM Cl− from 86% to less than 7%, making it a highly OER-selective catalyst. **b**, Top panel exhibits CVs of an IrO_x/GC rotating disk electrode in 0.5 M $KHSO_4$, 30 mM KCl (pH = 0.88), and 0.6 mM $MnSO_4$ (0 for the Mn^2+-free experiment). Rotation rate: 1500 rpm. MnO_x films were preconditioned at various times at 1.48 V before initiating the forward scan at 1.48 V. The inset shows the details of CVs for potentials between 1.2 and 1.5 V. The lower panel shows the corresponding i_{Ring} (E_{Ring} = 0.95 V). Figures adapted/reproduced with permission from ref. [64], American Chemical Society. RHE, reversible hydrogen electrode.

Cl^- blocking layer. In order to circumvent the overpotential limitations that are imposed by thermodynamics for a selective OER catalyst surface in the presence of Cl^- ions, an approach based on the application of a protecting MnO_x electrode coating was employed (Fig. 5a)[64]. The study on Mn based catalysts for saline water oxidation started with the report of MnO_2 on a dimensionally stable anode (DSA) obtaining OER selectivity of 99%[14]. γ-MnO_2 type multimetallic catalysts were investigated systematically for the OER- selective water oxidation in 0.5 M NaCl aqueous solution at various pH (1–10), with all of them showing efficiency higher than 90%. These catalysts included Mn–W[65], Mn–Mo[66–68], Mn–Mo–W[69–71], Mn–Mo–Fe[70,72] and Mn–Mo–S[73,74].

The electrode architecture consisted of Mn-based catalysts on iridium oxide coated Ti substrate electrodes. The purpose of the iridium oxide intermediate layer was the protection of the Ti substrate from the formation of insulating TiO_2. Rutile-type $Ir_{1-x}Sn_xO_2$ was found as the most effective intermediate layer[73], even though the oxidation of the Ti substrate could not be entirely prevented.

This led to an increased overpotential for $Mn_{1-x-y}Mo_xSn_yO_{2+x}$ after electrolysis for 1000 hours at 100 mA cm^{-2} in 0.5 M NaCl solution at pH 1[73,74]. A study on $Ir_{1-x}Sn_xO_2$ without coating of Mn-based catalysts confirmed that Ti oxidation is unavoidable, even though protection could be tuned by varying element composition and calcination temperature[75]. In these studies, the OER catalytically active phase is considered to be the Mn-based outer layer even though IrO_2 is an active OER catalyst.

A recent study showed MnO_x overlayers play the role of blocking the diffusion of Cl^- to the Ir-based intermediate layer, since iridium oxides are also known as excellent ClER catalysts[64]. Using an electrodeposited MnO_x thin film on glassy carbon-supported hydrous iridium oxide (IrO_x/GC) in

aqueous chloride solutions of pH ~0.9 (ref. [64]), the enhanced OER selectivity due to the presence of the MnO_x layer was confirmed in 30 mM Cl^- solution (Fig. 5b). It was concluded that MnO_x was not involved in the OER mechanism, but rather acted as a Cl^- diffusion barrier, while remaining permeable to water (Fig. 5a).

However, MnO_x is known to act as an OER catalyst itself, becoming OER active at somewhat more anodic potentials above +1.6 V versus RHE. Thus, it is feasible that at more anodic overpotentials the protecting MnO_x layer may not only become active for OER, but may also start catalysing the ClER[44]. This speculation, however, needs experimental validation. In addition, locally very acidic pH conditions at the MnO_x layer may lead to detrimental corrosion. The presented electrode performances of MnO_x coated electrodes are lower compared to the Mn-free IrO_x electrode (Fig. 5b), which could be due to the limited water diffusion through the catalytically inert MnO_x layer[64]. The use of such blocking layers should be optimized to prevent such negative effects from happening.

Another approach to suppress ClER involves coating OER catalysts such as $NiFeO_x$ and CoO_x with a permselective cerium oxide layer. This has allowed water oxidation to proceed whilst remaining impermeable to Cl^-, amongst other small ions and molecule contaminations[76]. Similarly, a cation-selective layer (Nafion) on IrO_x electrodes can prevent Cl^- ion from approaching the IrO_x electrode and improve the oxygen production (in a 0.5 M NaCl solution at pH 8.3)[77]. The advantage of this approach is the catalytic inertness of Nafion compared to MnO_x and CeO_x. Note that the operating cell voltages at 100 mA cm^{-2} were reported to be ~3.2 V greater compared to conventional alkaline water electrolysers, possibly due to the lower conductivity of NaCl solution compared to KOH solution.

Cathodes for H_2 evolution

In contrast to water oxidation at the anode, the primary concerns for the operation of a cathode in impure water do not relate to low Faradaic efficiencies, but are instead based upon the long-term stability of HER electrocatalysts in the presence of impurities which can lead to active site blocking and corrosion. Both saline and surface fresh water contain high levels of undesirable cationic species, including Ca^{2+} and Mg^{2+}, which are known to deposit at the cathode as hydroxides under reductive conditions, and current density losses of >50% have been reported due to salt deposition after short periods of operation (24 hours)[19,78]. The cathode surface can also be affected through reduction and electrodeposition of dissolved ions such as Cu, Cd, Sn and Pb under reaction conditions[79]. The extent to which competing cathode reactions involving metal cations occur will depend on the applied potential window and the specific ions present. Lab-scale studies typically use purified saline solutions (only NaCl) or electrolytes of known compositions. Further studies that address in detail the role of specific impurities such as salts or metals on electrode activity would be highly beneficial to the community.

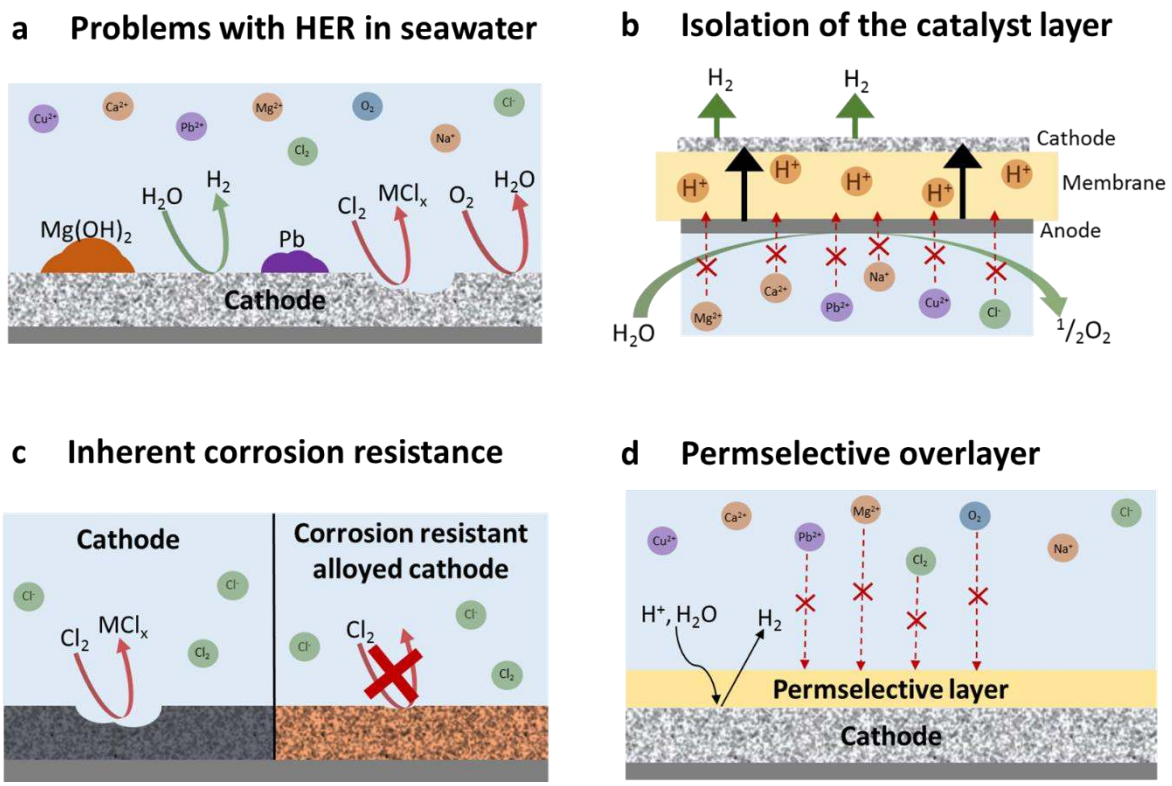

Fig. 6 Challenges and potential solutions to improve long-term stability of HER in low-grade water. a, Challenges for cathode operation in low-grade or saline water are in particular related to reduced stability due to deposition of impurities such as metal ions and hydroxides, and corrosion of the catalyst. **b**, Separation of the catalyst from the water source by a suitable membrane or through reactor design could prevent catalyst deactivation. **c**, Development of catalysts with inherent corrosion resistance or selective surface chemistry are desirable if long-term stability is to be maintained. **d**, Use of a permselective overlayer on top of the catalyst or on top of the membrane can prevent unwanted species from reaching the catalyst surface while also allowing normal catalytic function to occur.

The changing composition of both sea and surface fresh water worldwide represents a challenge when trying to pinpoint specific impurities and it would be beneficial for the community to agree on a standardized seawater composition for testing. Solid impurities and microbial contaminations that are not typically present in synthetic electrolytes also require attention and may lead to further reductions in activity by physically blocking the catalyst surface. Key approaches to improve stability at the cathode include the potential use of membranes to prevent impurities reaching the cathode through an engineering approach (for example, PEM electrolysers); the development of catalysts with surface sites selective to HER and resistant to side reactions/deactivation; and the deposition of permselective overlayers on top of the catalyst to block impurities whilst allowing the transfer of reagents and products.

pH design criterion. Pt is currently regarded as the benchmark HER electrocatalyst, in both acid and alkali conditions. Plots of catalytic rate versus metal–hydrogen (M–H) binding energy (volcano plots[80]) show that Pt achieves a near optimal level of activity leading to it being the common choice for PEMWE where an acidic environment is provided by the membrane[9,25]. However the cost of Pt is high and alkaline electrolysers typically use Ni or Ni-based metal alloys (such as NiMo, NiMoCo and NiFe) for

the HER due to their lower cost and stability at low pH environments[9,25,63]. There is a significant interest in the development of new H_2 evolution electrocatalysts to act as cost effective alternatives to expensive catalysts such as Pt[81]. We refer the reader to recent studies highlighting the range of high-performance electrocatalysts for HER identified in recent years covering a wide operating pH range[39,63]. In almost all cases these examples have yet to be tested in low-grade or saline water.

From the perspective of cathode performance, PEMWE provides an optimal pH for HER due to the high local concentration of H^+ supplied by the membrane[29]. A PEMWE configuration could also protect the cathode from impurities by acting as a filtration barrier as depicted in Fig. 6b, provided a highly selective membrane can be found. However, a PEMWE configuration provides a minimal overpotential window and does not satisfy the OER operation conditions for avoiding Cl_2 production at the anode. Given that a successful saline water splitting device will likely have to operate in near neutral to alkaline (pH > 8) conditions the following discussions focus on neutral to alkali HER catalysis. Finding HER catalysts which can operate efficiently in neutral to alkaline conditions also provides an opportunity to target cheaper earth abundant elements such as Ni, Mn and Fe, which are typically unstable in acidic conditions[82].

HER catalyst selectivity and stability. Table 1 provides a summary of HER electrodes that have been tested for low-grade, saline or seawater. The studies presented in Table 1 have assessed their systems using different criteria and as such direct comparison is difficult. This highlights the need for standard criteria when assessing potential catalysts in seawater applications.

It is notable that many of the cathodes reported in Table 1 have focused on using saline water at/near neutral pH; exceptions include Pt, Ni–Fe–C and FeO_x cathodes that have been tested in alkaline media in the presence of Cl^-. Pt has been operated as a cathode in an alkaline electrolyser containing 0.5 M NaCl[21]. A loss of current density of ~50% was reported after 100 hours of continuous operation. This loss was proposed to be due to deterioration of the alkali membrane conductivity rather than catalyst deactivation. A 4-hour rest period every 20 hours was found to lead to a recovery effect. The system was not tested in real seawater, however the results in NaCl did not indicate cathode failure. A carbon content and grain size study of Ni–Fe–C electrodes[83] was carried out in electrolyte containing 3.5% NaCl solution at 90 ºC and pH = 12. The electrocatalysts with the maximum carbon content (1.59%) and minimum grain size (3.4 nm) was shown to possess the lowest overpotential for HER.

Table 1: H_2 evolution electrocatalysts reported in saline electrolyte

Catalyst	Support	Electrolyte	Cell setup	Ref
Pt	Pt plate	Neutral phosphate buffered natural seawater.	1-compartment, 2-electrode cell with IrO_2 on carbon cloth counter electrode.	62

Pt nanoparticles: Pt 46.7 wt% with carbon black	Spray coated onto Tokuyama A201 membrane	0.1 M KOH + 0.5 M NaCl.	Membrane electrode assembly with Ni-Fe layered double hydroxide anode material spray coated onto reverse.	21
NiMoS	Carbon fibre cloth	Neutral phosphate buffered natural seawater.	1-compartment, 2-electrode cell with MHCM-z-BCC counter electrode.	62
Nanostructured NiMoS	Carbon fibre cloth	Natural seawater, pH = 8.07.	1-compartment, 3-electrode cell with graphite foil counter electrode.	85
Ni-M (M¼ Co, Cu, Mo, Au, Pt)	Ti mesh	Natural seawater, filtered to remove large particulates.	3-electrode system with Pt sheet counter electrode and Ag/AgCl reference electrode.	89
Pt-M (M¼ Cr, Fe, Co, Ni, Mo)	Ti mesh	Natural seawater.	3-electrode system with a platinum sheet counter electrode and Ag/AgCl reference electrode.	90
FeO_x	FTO glass slide	0.6 M NaCl + 0.1 M KOH, pH = 13.	2-electrode, 2-compartment setup, FeOx counter-reference electrode, Nafion® 117 membrane.	103
Mn doped NiO/Ni	Ni-foam	Natural seawater, pH = 8.2.	1-compartment, 3-electrode cell with graphite rod counter electrode and SCE reference electrode.	78
Urea-derived carbon nanotubes	Drop-cast onto glassy carbon electrode	Natural seawater with phosphate buffer, pH=7.	1-compartment, 3-electrode cell with carbon rod counter electrode and SCE reference electrode.	104
CoMoP with 2-4 layer graphitic carbon shell	Drop cast onto glassy carbon electrode	Natural seawater, filtered, pH = 8.35.	1-compartment, 3-electrode configuration with graphite rod counter electrode and SCE reference electrode.	105
Ni-Fe-C	Etched steel substrate	3.5% NaCl solution at 90 °C, pH = 12.	1-compartment, 3 electrode cell with Pt plate counter electrode and Hg/HgO (1 M NaOH) reference electrode.	84
CoSe and Co_9Se_8	Cobalt foil	Phosphate buffered natural seawater.	1 compartment, 3-electrode cell with carbon counter electrode and Ag/AgCl reference electrode.	49
Co_3Mo_3C/carbon nano tubes	Ni foam	Natural seawater, filtered.	3-electrode cell, 1-compartment, with platinum sheet counter electrode and Ag/AgCl reference electrode.	106
Mo_5N_6	Drop-cast onto glassy carbon	Natural seawater, pH~8.4.	3-electrode cell, 1-compartment, Graphite rod counter electrode and Ag/AgCl reference electrode, constant flow of Ar to remove gas build up.	107
Co-S	FTO glass slide	Natural seawater with 1 M $NaClO_4$.	3-electrode, medium frit separated 2-compartment cell, with FTO counter electrode and Ag/AgCl reference electrode.	108

NiNS	Ni foam	Natural seawater with phosphate buffer, pH = 7.05.	2-electrode cell with NiNS as anode and cathode.	109

Bifunctional catalysts capable of operating as both anode and cathode are attractive as this simplifies cell construction, and could also allow for electrochemical regeneration by potential switching as in the case of FeO_x bi-functional material in KOH (pH = 13)[41]. Reversing the anode and cathode every 1 hour by potential switching prevents (entirely within error) catalyst activation loss[41]. Similar results were achieved for iron foil electrodes, in which addition of 0.6 M NaCl to the system revealed quantitative water splitting with 2:1 generation of H_2:O_2, however testing was not carried out in real seawater.

Earth abundant HER catalysts[82] have recently been reported for electrolysis in neutral media. Catalysts consisting of a Cu surface modified by Ni atoms and CrO_x clusters were prepared through anisotropic doping of the metal surface and have been proposed to asymmetrically destabilize bonds in the water molecule to favour its dissociation into H^+ and OH^-. NiMoS has been evaluated and proposed as a potential cathode material for operation in saline water at neutral pH[62,84]. When combined with a MHCM–*z*–BCC anode the system operated for 100 hours in neutral buffered saline water with minimal current density decline.

Corrosion due to Cl^- and related Cl^- oxidation products such as Cl_2 can be a concern for electrode stability. While chloride oxidation products are primarily a concern for the anode, gas crossover is possible,[85] and the stability of the cathode in the presence of chloride and oxidation products such as Cl_2 should be carefully considered. Crossover can be managed to an extent by controlling membrane thickness to find a suitable balance between separation properties and conductivity, and by controlling pressure gradients. Alloys of either Pt or Ni with transition metals including Cr, Fe, Co and Mo (that is, PtM and NiM) have been shown to reduce corrosion leading to metal chloride formation in saline water and in the presence of Cl_2, increasing long-term stability[86–89]. PtMo (ref. [89]) and PtRuMo (ref. [86]) alloys on Ti mesh have shown excellent performance in real seawater with <10% loss of their original current density after 172 hours of operation. NiMo (refs. [87,88]) alloys have also been shown to provide a promising combination of catalytic activity and longterm stability. The increased corrosion resistance of these alloys is attributed to competitive dissolution reactions between the guest M species with Cl_2 (ref. [86]). Alloys containing Mo are also widely reported in more traditional water splitting applications to possess favourable overpotentials and stability[63,90]. Development of catalysts capable of inherently resisting corrosion or poisoning due to foreign ion deposition such as those described above are desirable in order to achieve long-term stability as exemplified in Fig. 6c.

Blocking layers. Addition of permselective barrier layers on catalyst surfaces has been demonstrated to limit unwanted Cl^- chemistry at the anode[91], and a similar approach could be envisaged for protecting cathode materials to enhance long-term stability, as shown in Fig. 6d. Several examples of cathode protecting layers have been demonstrated recently. A thin layer of $Cr(OH)_3$ coated onto a Pt cathode

has been reported to act as a selective blocking layer, providing selectivity for the HER over competing hypochlorate reduction in the chlorate process[92,93]. MnO_x has also been suggested to play a similar role to that of $Cr(OH)_3$[64,94]. A graphitic shell around a CoMoP electrocatalyst has been shown to promote HER performance and provide protection against etching, agglomeration and poisoning in saline water[95]. Furthermore, it is possible that permselective layers could play a dual role in electrolyser systems, by protecting both the catalyst layer and also any membrane which sits underneath the catalyst. Although mass transport issues may arise upon the addition of a permselective overlayer, such an approach could provide a significant improvement to the long-term stability of a system operating in impure water.

Conclusions and outlook

Several issues need attention for electrolysis of impure or saline water to become viable. The use of appropriate membranes is crucial for building an efficient electrolyser using seawater or lowgrade water without extensive purification/treatments. Common membrane and diaphragm technologies are susceptible to transport of and blockage by foreign ions, however the effect this has on the activity and longevity of a system is not fully understood and further research into membrane blockage by impurities would be highly valuable.

At the anode, overcoming the competition between chlorine chemistry and water oxidation is essential for successful saline water splitting. Oxygen evolution selectivity can be obtained by operating in alkaline conditions, and this has been demonstrated in highly alkaline systems (pH ~13) containing NaCl. However, a transition to real seawater at high pH is expected to have additional challenges associated with precipitation formation when seawater is adjusted to pH greater than ~10 (ref. [18]). Based on the Pourbaix diagram, there may be an opportunity to operate near pH 8–9 and maintain O_2 selectivity. In this scenario, careful control of pH becomes a vital task and a strong buffer is likely required. Other strategies for operating anodes and cathodes in impure water include selective transport of ions by membranes, formation of permselective materials/ barriers onto the surface of catalysts, and finding electrode materials with catalytically selective sites to favour desired reactions over side-reactions and catalysts poisoning.

It would be beneficial for the community to assess new materials for use in impure water using standardized criteria. The composition of real seawater is complex and varies around the globe, and the use of a standardized electrolyte composition (for example, Instant Ocean) for benchmarking new catalyst materials is important. For buffered saline water, a similar standard should be employed along with a clearly defined nature and concentration of the buffer species. Other relevant parameters that need standardization include long-term stability assessment (>100 hours) at a standard current density (10 mA cm^{-2} in batch systems, 200 mA cm^{-2} in flow electrolysis cells).

Some electrocatalysts are already available with good activity and selectivity[24,92], but long-term stability remains an issue. For membranes, an interesting approach could be to mimic electrokinetic membranes found in certain plants such as mangrove roots that filter seawater, thereby reducing saline concentration on the surface of the electrode, and minimize membrane fouling or decomposition[96].

The transformation towards a decarbonized society requires careful considerations in reducing the cost. In most cases, saline water electrolyser technologies will need to have competitive capital and operational costs (CAPEX and OPEX) compared to electrolyser technologies coupled to desalination and purification units. Extra revenue may be obtainable if a careful management of the waste stream is utilized[97]. We believe that islands can be ideal places to test new technologies given the abundance of renewable energy and the desire for storage and self-sufficiency[98], combined with the inherent current costs of importing fossil fuels not available in these territories. Although it remains unclear which of the electrolyser technologies will be more suitable for saline waters, the operation at near neutral pH (7–9) is preferable and AEM would most likely fulfil this requirement, unless gas-phase electrolysis becomes competitive.

References

1. Vörösmarty, C. J. et al. Global threats to human water security and river biodiversity. *Nature* **467**, 555–561 (2010).
2. Spröte, W. in *A Concise Encyclopedia of the United Nations* Vol. 07404 (ed Volger, H.) 147–152 (Brill, 2010).
3. *The Future of Hydrogen* (International Energy Agency, 2019).
4. Bezdek, R. H. The hydrogen economy and jobs of the future. *Renew. Energy Environ. Sustain.* **4**, 1 (2019).
5. Moliner, R., Lázaro, M. J. & Suelves, I. Analysis of the strategies for bridging the gap towards the Hydrogen Economy. *Int. J. Hydrog. Energy* **41**, 19500–19508 (2016).
6. Deutsch, T. G. & Turner, J. A. *Semiconductor Materials for Photoelectrolysis: 2014 Annual Progress Report U. S. DOE Hydrogen & Fuel Cells Program* (Department of Energy, 2014).
7. Ramsden, T., Ruth, M., Diakov, V., Laffen, M. & Timbario, T. A. *Hydrogen Pathways: Updated Cost, Well-to-Wheels Energy Use, and Emissions for the Current Technology Status of Ten Hydrogen Production, Delivery, and Distribution Scenarios* (National Renewable Energy Laboratory, 2013).
8. Ursúa, A., Gandía, L. M. & Sanchis, P. Hydrogen production from water electrolysis: current status and future trends. *Proc. IEEE* **100**, 410–426 (2012).
9. Xiang, C., Papadantonakis, K. M. & Lewis, N. S. Principles and implementations of electrolysis systems for water splitting. *Mater. Horiz.* **3**, 169–173 (2016).
10. Matute, G., Yusta, J. M. & Correas, L. C. Techno-economic modelling of water electrolysers in the range of several MW to provide grid services while generating hydrogen for different applications: a case study in Spain applied to mobility with FCEVs. *Int. J. Hydrog. Energy* **44**, 17431–17442 (2019).
11. Chardonnet, C. et al. *Study on Early Business Cases for H_2 in Energy Storage and More Broadly Power To H2 Applications* (EU Commission, 2017).
12. Karagiannis, I. C. & Soldatos, P. G. Water desalination cost literature: review and assessment. *Desalination* **223**, 448–456 (2008).
13. Fourmond, V., Jacques, P. A., Fontecave, M. & Artero, V. H_2 evolution and molecular electrocatalysts: Determination of Overpotentials and effect of homoconjugation. *Inorg. Chem.* **49**, 10338–10347 (2010).
14. Bennett, J. E. Electrodes for generation of hydrogen and oxygen from seawater. *Int. J. Hydrog. Energy* **5**, 401–408 (1980).
15. Katsounaros, I. et al. The effective surface pH during reactions at the solid-liquid interface. *Electrochem. commun.* **13**, 634–637 (2011).
16. Auinger, M. et al. Near-surface ion distribution and buffer effects during electrochemical reactions. *Phys. Chem. Chem. Phys.* **13**, 16384–16394 (2011).
17. Dionigi, F., Reier, T., Pawolek, Z., Gliech, M. & Strasser, P. Design criteria, operating conditions, and nickel-iron hydroxide catalyst materials for selective seawater electrolysis. *ChemSusChem* **9**, 962–972 (2016).

18. Kapp, E. M. The precipitation of calcium and magnesium from sea water by sodium hydroxide. *Biol. Bull.* **55**, 453–458 (1928).
19. Kirk, D. W. & Ledas, A. E. Precipitate formation during sea water electrolysis. *Int. J. Hydrog. Energy* **7**, 925–932 (1982).
20. Dresp, S. & Strasser, P. Non-noble metal oxides and their application as bifunctional catalyst in reversible fuel cells and rechargeable air batteries. *ChemCatChem* **10**, 4162–4171 (2018).
21. Dresp, S. et al. Direct electrolytic splitting of seawater: activity, selectivity, degradation, and recovery studied from the molecular catalyst structure to the electrolyzer cell level. *Adv. Energy Mater.* **8**, 1800338 (2018).
22. Adbel-Aal, H. K. & Hussein, I. A. Parametric study for saline water electrolysis: part 1-hydrogen production. *Int. J. Hydrog. Energy* **18**, 485–489 (1993).
23. Oh, B. S. et al. Formation of hazardous inorganic by-products during electrolysis of seawater as a disinfection process for desalination. *Sci. Total Environ.* **408**, 5958–5965 (2010).
24. Dresp, S., Dionigi, F., Klingenhof, M. & Strasser, P. Direct electrolytic splitting of seawater: opportunities and challenges. *ACS Energy Lett.* **4**, 933–942 (2019).
25. Carmo, M., Fritz, D. L., Mergel, J. & Stolten, D. A comprehensive review on PEM water electrolysis. *Int. J. Hydrog. Energy* **38**, 4901–4934 (2013).
26. Vincent, I. & Bessarabov, D. Low cost hydrogen production by anion exchange membrane electrolysis: A review. *Renew. Sustain. Energy Rev.* **81**, 1690–1704 (2018).
27. Meng, Y. et al. Review: recent progress in low-temperature protonconducting ceramics. *J. Mater. Sci.* **54**, 9291–9312 (2019).
28. Laguna-Bercero, M. A. Recent advances in high temperature electrolysis using solid oxide fuel cells: a review. *J. Power Sources* **203**, 4–16 (2012).
29. Mauritz, K. A. & Moore, R. B. State of understanding of Nafion. *Chem. Rev.* **104**, 4535–4586 (2004).
30. Chae, K. J. et al. Mass transport through a proton exchange membrane (Nafion) in microbial fuel cells. *Energy Fuels* **22**, 169–176 (2008).
31. Müller, M. et al. Water management in membrane electrolysis and options for advanced plants. *Int. J. Hydrog. Energy* **44**, 10147–10155 (2019).
32. Schalenbach, M., Lueke, W. & Stolten, D. Hydrogen diffusivity and electrolyte permeability of the Zirfon PERL separator for alkaline water electrolysis. *J. Electrochem. Soc.* **163**, 1480–1488 (2016).
33. Lim, C. K., Liu, Q., Zhou, J., Sun, Q. & Chan, S. H. High-temperature electrolysis of synthetic seawater using solid oxide electrolyzer cells. *J. Power Sources* **342**, 79–87 (2017).
34. Hine, F., O'Brien, T. F. & Bommaraju, T. V. *Handbook of Chlor-alkali Technology, Volume I: Fundamentals* (Springer, 2005).
35. Karlsson, R. K. B. & Cornell, A. Selectivity between oxygen and chlorine evolution in the chlor-alkali and chlorate processes. *Chem. Rev.* **116**, 2982–3028 (2016).
36. Kumari, S., Turner White, R., Kumar, B. & Spurgeon, J. M. Solar hydrogen production from seawater vapor electrolysis. *Energy Environ. Sci.* **9**, 1725–1733 (2016).
37. Heremans, G. et al. Vapor-fed solar hydrogen production exceeding 15% efficiency using earth abundant catalysts and anion exchange membrane. *Sustain. Energy Fuels* **1**, 2061–2065 (2017).
38. Kida, T. et al. Water vapor electrolysis with proton-conducting graphene oxide nanosheets. *ACS Sustain. Chem. Eng.* **6**, 11753–11758 (2018).
39. McCrory, C. C. L. et al. Benchmarking hydrogen evolving reaction and oxygen evolving reaction electrocatalysts for solar water splitting devices. *J. Am. Chem. Soc.* **137**, 4347–4357 (2015).
40. Gong, M. et al. An advanced Ni–Fe layered double hydroxide electrocatalyst for water oxidation. *J. Am. Chem. Soc.* **135**, 8452–8455 (2013).
41. Martindale, B. C. M. & Reisner, E. Bi-functional iron-only electrodes for efficient water splitting with enhanced stability through in situ electrochemical regeneration. *Adv. Energy Mater.* **6**, 1502095 (2016).
42. Huang, W.-H. & Lin, C.-Y. Iron phosphate modified calcium iron oxide as an efficient and robust catalyst in electrocatalyzing oxygen evolution from seawater. *Faraday Discuss.* **215**, 205–215 (2019).
43. Juodkazytė, J. et al. Electrolytic splitting of saline water: durable nickel oxide anode for selective oxygen evolution. *Int. J. Hydrog. Energy* **44**, 5929–5939 (2019).
44. Trasatti, S. Electrocatalysis in the anodic evolution of oxygen and chlorine. *Electrochim. Acta* **29**, 1503–1512 (1984).
45. Hansen, H. A. et al. Electrochemical chlorine evolution at rutile oxide (110) surfaces. *Phys. Chem. Chem. Phys.* **12**, 283–290 (2010).
46. Exner, K. S., Anton, J., Jacob, T. & Over, H. Controlling selectivity in the chlorine evolution reaction over RuO_2-based catalysts. *Angew. Chem. Int. Ed.* **53**, 11032–11035 (2014).
47. Surendranath, Y. & Dinca, M. Electrolyte-dependent electrosynthesis and activity of cobalt-based water oxidation catalysts. *J. Am. Chem. Soc.* **131**, 2615–2620 (2009).

48. Cheng, F. et al. Synergistic action of Co-Fe layered double hydroxide electrocatalyst and multiple ions of sea salt for efficient seawater oxidation at near-neutral pH. *Electrochim. Acta* **251**, 336–343 (2017).
49. Zhao, Y. et al. Charge state manipulation of cobalt selenide catalyst for overall seawater electrolysis. *Adv. Energy Mater.* **8**, 1801926 (2018).
50. Zeradjanin, A. R., Menzel, N., Schuhmann, W. & Strasser, P. On the faradaic selectivity and the role of surface inhomogeneity during the chlorine evolution reaction on ternary Ti-Ru-Ir mixed metal oxide electrocatalysts. *Phys. Chem. Chem. Phys.* **16**, 13741–13747 (2014).
51. Macounová, K., Makarova, M., Jirkovský, J., Franc, J. & Krtil, P. Parallel oxygen and chlorine evolution on Ru1-xNixO2-y nanostructured electrodes. *Electrochim. Acta* **53**, 6126–6134 (2008).
52. Kishor, K., Saha, S., Parashtekar, A. & Pala, R. G. S. Increasing chlorine selectivity through weakening of oxygen adsorbates at surface in Cu doped RuO_2 during seawater electrolysis. *J. Electrochem. Soc.* **165**, J3276–J3280 (2018).
53. Arikawa, T., Murakami, Y. & Takasu, Y. Simultaneous determination of chlorine and oxygen evolving at RuO2/Ti and RuO2-TiO2/Ti anodes by differential electrochemical mass spectroscopy. *J. Appl. Electrochem.* **28**, 511–516 (1998).
54. Karlsson, R. K. B., Hansen, H. A., Bligaard, T., Cornell, A. & Pettersson, L. G. M. Ti atoms in $Ru_{0.3}Ti_{0.7}O_2$ mixed oxides form active and selective sites for electrochemical chlorine evolution. *Electrochim. Acta* **146**, 733–740 (2014).
55. Exner, K. S., Anton, J., Jacob, T. & Over, H. Chlorine evolution reaction on ruo2 (110): ab initio atomistic thermodynamics study - Pourbaix diagrams. *Electrochim. Acta* **120**, 460–466 (2014).
56. Sohrabnejad-Eskan, I. et al. Temperature-dependent kinetic studies of the chlorine evolution reaction over RuO_2(110) model electrodes. *ACS Catal.* **7**, 2403–2411 (2017).
57. Petrykin, V., Macounova, K., Shlyakhtin, O. A. & Krtil, P. Tailoring the selectivity for electrocatalytic oxygen evolution on ruthenium oxides by zinc substitution. *Angew. Chem. Int. Ed.* **49**, 4813–4815 (2010).
58. Nong, H. N. et al. A unique oxygen ligand environment facilitates water oxidation in hole-doped $IrNiO_x$ core–shell electrocatalysts. *Nat. Catal.* **1**, 841–851 (2018).
59. Bergmann, A. et al. Unified structural motifs of the catalytically active state of Co(oxyhydr)oxides during the electrochemical oxygen evolution reaction. *Nat. Catal.* **1**, 711–719 (2018).
60. Beermann, V. et al. Real-time imaging of activation and degradation of carbon supported octahedral Pt–Ni alloy fuel cell catalysts at the nanoscale using in situ electrochemical liquid cell STEM. *Energy Environ. Sci.* **12**, 2476–2485 (2019).
61. Fabbri, E., Abbott, D. F., Nachtegaal, M. & Schmidt, T. J. Operando X-ray absorption spectroscopy: a powerful tool toward water splitting catalyst development. *Curr. Opin. Electrochem.* **5**, 20–26 (2017).
62. Hsu, S.-H. et al. An earth-abundant catalyst-based seawater photoelectrolysis system with 17.9% solar-to-hydrogen efficiency. *Adv. Mater.* **30**, 1707261 (2018).
63. Zeng, M. & Li, Y. Recent advances in heterogeneous electrocatalysts for the hydrogen evolution reaction. *J. Mater. Chem. A* **3**, 14942–14962 (2015).
64. Vos, J. G., Wezendonk, T. A., Jeremiasse, A. W. & Koper, M. T. M. MnO_x/ IrO_x as selective oxygen evolution electrocatalyst in acidic chloride solution. *J. Am. Chem. Soc.* **140**, 10270–10281 (2018).
65. Izumiya, K. et al. Anodically deposited manganese oxide and manganesetungsten oxide electrodes for oxygen evolution from seawater. *Electrochim. Acta* **43**, 3303–3312 (1998).
66. Fujimura, K. et al. Anodically deposited manganese-molybdenum oxide anodes with high selectivity for evolving oxygen in electrolysis of seawater. *J. Appl. Electrochem.* **29**, 765–771 (1999).
67. Fujimura, K. et al. Oxygen evolution on manganese-molybdenum oxide anodes in seawater electrolysis. *Mater. Sci. Eng. A* **267**, 254–259 (1999).
68. Fujimura, K. et al. The durability of manganese–molybdenum oxide anodes for oxygen evolution in seawater electrolysis. *Electrochim. Acta* **45**, 2297–2303 (2000).
69. El-Moneim, A. A., Kumagai, N., Asami, K. & Hashimoto, K. New nanocrystallinemanganese-molybdenum-tin oxdie anodes for oxygen evolution in seatwater electrolysis. *ECS Trans.* **1**, 491–497 (2006).
70. Matsui, T. et al. Anodically deposited Mn-Mo-W oxide anodes for oxygen evolution in seawater electrolysis. *J. Appl. Electrochem.* **32**, 993–1000 (2002).
71. El-Moneim, A. A. Mn-Mo-W-oxide anodes for oxygen evolution during seawater electrolysis for hydrogen production: effect of repeated anodic deposition. *Int. J. Hydrog. Energy* **36**, 13398–13406 (2011).
72. Abdel Ghany, N. A., Kumagai, N., Meguro, S., Asami, K. & Hashimoto, K. Oxygen evolution anodes composed of anodically deposited Mn-Mo-Fe oxides for seawater electrolysis. *Electrochim. Acta* **48**, 21–28 (2002).
73. Kato, Z., Bhattarai, J., Kumagai, N., Izumiya, K. & Hashimoto, K. Durability enhancement and degradation of oxygen evolution anodes in seawater electrolysis for hydrogen production. *Appl. Surf. Sci.* **257**, 8230–8236 (2011).

74. Kato, Z. et al. Electrochemical characterization of degradation of oxygen evolution anode for seawater electrolysis. *Electrochim. Acta* **116**, 152–157 (2014).
75. Kato, Z. et al. The influence of coating solution and calcination condition on the durability of $Ir_{1-x}Sn_xO_2$/Ti anodes for oxygen evolution. *Appl. Surf. Sci.* **388**, 640–644 (2016).
76. Obata, K. & Takanabe, K. A Permselective CeO_x coating to improve the stability of oxygen evolution electrocatalysts. *Angew. Chem. Int. Ed.* **57**, 1616–1620 (2018).
77. Balaji, R. et al. An alternative approach to selective sea water oxidation for hydrogen production. *Electrochem. commun.* **11**, 1700–1702 (2009).
78. Lu, X. et al. A sea-change: manganese doped nickel/nickel oxide electrocatalysts for hydrogen generation from seawater. *Energy Environ. Sci.* **11**, 1898–1910 (2018).
79. Bard, A. J., Parsons, R. & Jordan, J. *Standard Potentials in Aqueous Solution* (Routledge, 1985).
80. Nørskov, J. K. et al. Trends in the exchange current for hydrogen evolution. *J. Electrochem. Soc.* **152**, J23 (2005).
81. Zheng, Y., Jiao, Y., Jaroniec, M. & Qiao, S. Z. Advancing the electrochemistry of the hydrogen-evolution reaction through combining experiment and theory. *Angew. Chem. Int. Ed.* **54**, 52–65 (2015).
82. Dinh, C.-T. et al. Multi-site electrocatalysts for hydrogen evolution in neutral media by destabilization of water molecules. *Nat. Energy* **4**, 107–114 (2019).
83. Song, L. J. & Meng, H. M. Effect of carbon content on Ni-Fe-C electrodes for hydrogen evolution reaction in seawater. *Int. J. Hydrog. Energy* **35**, 10060–10066 (2010).
84. Miao, J. et al. Hierarchical Ni-Mo-S nanosheets on carbon fiber cloth: A flexible electrode for efficient hydrogen generation in neutral electrolyte. *Sci. Adv.* **1**, e1500259 (2015).
85. Schalenbach, M. et al. Gas permeation through nafion. Part 1: measurements. *J. Phys. Chem. C.* **119**, 25145–25155 (2015).
86. Li, H., Tang, Q., He, B. & Yang, P. Robust electrocatalysts from an alloyed Pt-Ru-M (M = Cr, Fe, Co, Ni, Mo)-decorated Ti mesh for hydrogen evolution by seawater splitting. *J. Mater. Chem. A* **4**, 6513–6520 (2016).
87. Golgovici, F. et al. Ni–Mo alloy nanostructures as cathodic materials for hydrogen evolution reaction during seawater electrolysis. *Chem. Pap.* **72**, 1889–1903 (2018).
88. Zhang, Y., Li, P., Yang, X., Fa, W. & Ge, S. High-efficiency and stable alloyed nickel based electrodes for hydrogen evolution by seawater splitting. *J. Alloy. Compd.* **732**, 248–256 (2018).
89. Zheng, J., Zhao, Y., Xi, H. & Li, C. Seawater splitting for hydrogen evolution by robust electrocatalysts from secondary M (M = Cr, Fe, Co, Ni, Mo) incorporated Pt. *RSC Adv.* **8**, 9423–9429 (2018).
90. Raj, I. A. & Vasu, K. I. Transition metal-based hydrogen electrodes in alkaline solution — electrocatalysis on nickel based binary alloy coatings. *J. Appl. Electrochem.* **20**, 32–38 (1990).
91. Esposito, D. V. Membrane-coated electrocatalysts - an alternative approach to achieving stable and tunable electrocatalysis. *ACS Catal.* **8**, 457–465 (2018).
92. Vos, J. G. & Koper, M. T. M. Measurement of competition between oxygen evolution and chlorine evolution using rotating ring-disk electrode voltammetry. *J. Electroanal. Chem.* **819**, 260–268 (2018).
93. Lindbergh, G. & Simonsson, D. The effect of chromate addition on cathodic reduction of hypochlorite in hydroxide and chlorate solutions. *J. Electrochem. Soc.* **137**, 3094–3099 (2006).
94. Endrődi, B. et al. Towards sustainable chlorate production: The effect of permanganate addition on current efficiency. *J. Clean. Prod.* **182**, 529–537 (2018).
95. Ma, Y. Y. et al. Highly efficient hydrogen evolution from seawater by a low-cost and stable CoMoP@C electrocatalyst superior to Pt/C. *Energy Environ. Sci.* **10**, 788–798 (2017).
96. Kim, K., Kim, H., Lim, J. H. & Lee, S. J. Development of a desalination membrane bioinspired by mangrove roots for spontaneous filtration of sodium ions. *ACS Nano* **10**, 11428–11433 (2016).
97. Kumar, A., Phillips, K. R., Thiel, G. P., Schröder, U. & Lienhard, J. H. Direct electrosynthesis of sodium hydroxide and hydrochloric acid from brine streams. *Nat. Catal.* **2**, 106–113 (2019).
98. Schiermeier, Q., Tollefson, J., Scully, T., Witze, A. & Morton, O. Energy alternatives: electricity without carbon. *Nature* **454**, 816–823 (2008).
99. Gao, S. et al. Electrocatalytic H_2 production from seawater over Co, N-codoped nanocarbons. *Nanoscale* **7**, 2306–2316 (2015).
100. Ma, Y. Y. et al. Highly efficient hydrogen evolution from seawater by a low-cost and stable CoMoP@C electrocatalyst superior to Pt/C. *Energy Environ. Sci.* **10**, 788–798 (2017).
101. Zhao, Y., Tang, Q., He, B. & Yang, P. Carbide decorated carbon nanotube electrocatalyst for high-efficiency hydrogen evolution from seawater. *RSC Adv.* **6**, 93267–93274 (2016).
102. Jin, H. et al. Single-crystal nitrogen-rich two-dimensional Mo_5N_6 nanosheets for efficient and stable seawater splitting. *ACS Nano* **12**, 12761–12769 (2018).
103. Sun, Y. et al. Electrodeposited cobalt-sulfide catalyst for electrochemical and photoelectrochemical hydrogen generation from water. *J. Am. Chem. Soc.* **135**, 17699–17702 (2013).

104. Zhao, Y., Jin, B., Vasileff, A., Jiao, Y. & Qiao, S. Interfacial nickel nitride/ sulfide as a bifunctional electrode for highly efficient overall water/seawater electrolysis. *J. Mater. Chem. A* **7**, 8117–8121 (2019).

Acknowledgements

W.T., M.F., R.S.E., A.J.C. and P.F. acknowledge financial support from INTERREG Atlantic Area programme (Grant reference EAPA_190_2016). P.F. acknowledges support from Royal Society Alumni programme. F.D., S.D. and P.S. gratefully acknowledge financial support by the German Research Foundation (DFG) through Grant reference number STR 596/8-1 and the federal ministry for economic affairs and energy (Bundesministerium für Wirtschaft und Energie, BMWi) under grant number 03EIV041F. P.S. acknowledges partial funding by the Deutsche Forschungsgemeinschaft (DFG, German Research Foundation) under Germany´s Excellence Strategy – EXC 2008/1 – 390540038 (zum Teil gefördert durch die Deutsche Forschungsgemeinschaft (DFG) im Rahmen der Exzellenzstrategie des Bundes und der Länder – EXC 2008/1 – 390540038).